FLYGTEKNISKA FÖRSÖKSANSTALTEN

THE AERONAUTICAL RESEARCH INSTITUTE OF SWEDEN

MEDDELANDE 108

REPORT 108

# CREEP DEFORMATION AND BUCKLING OF A CIRCULAR CYLINDRICAL SHELL UNDER AXIAL COMPRESSION

by

*Åke Samuelson*

## SUMMARY

In a recent paper, FFA Report No. 100, a theory of elastic deformation and secondary creep of a circular cylindrical shell under axisymmetrical loads was derived, and an approximate criterion for buckling was proposed. The theory was based on the "*l*-membrane" analogy, and numerical solutions were derived for the special case of a "double-membrane" shell. In the present report, the general equations were solved for an arbitrary, odd number of membranes and the results were compared with those of the previous report.

It was found that the double-membrane analogy yields an over-estimate of the deflection and stress rates, but the effect on the creep buckling time as calculated from the approximate method was small in comparison with the scatter normally obtained at creep buckling tests. Therefore, the double-membrane shell was found to provide sufficiently accurate results for practical use. However, if a higher degree of accuracy is wanted, the 3-flange model was found to yield a very close approximation to the solution provided by a multi-membrane shell.

A few creep buckling experiments were carried out on thin aluminium-alloy cylinders under various stress levels. The number of circumferential lobes developed on collapse was found to decrease with a decreasing load level, and at a very low axial mean stress an axisymmetrical buckling configuration was noted.

The approximate buckling condition proposed in FFA Report No. 100 was applied to the test cylinders and fairly good agreement with the experimental results was found.

Stockholm, November 1966

---

# KRIECHVERHALTEN UND AUSBEULEN EINES KREISZYLINDERS UNTER AXIALER DRUCKBELASTUNG

von

*Åke Samuelson*

## ZUSAMMENFASSUNG

In einem früheren Bericht, FFA Nr. 100, wurde eine Theorie einer elastischen Verformung und sekundären Kriechens an einer Kreiszylinderschale bei axisymmetrischen Belastungen aufgestellt und ein Näherungsverfahren für die Verbeulung angegeben. Die Theorie baute auf der „*l*-Membran"-Analogie. Für den besonderen Fall der „Doppelmembranschale" wurden ziffernmässige Lösungen gegeben. In dem gegenwärtigen Bericht werden die allgemeinen Gleichungen für eine beliebig gewählte ungerade Anzahl von Membranen gelöst und die Ergebnisse mit denen des früheren Berichts verglichen.

Es ergab sich, dass die Doppelmembran-Analogie eine Überbewertung der Verformungsänderung und der Beanspruchung liefert. Die Wirkung auf die Kriechbeulungszeit, wie in dem Näherungsverfahren berechnet, war aber im Verhältnis zu der normalerweise bei Kriechbeulungsversuchen erhaltenen Streuung gering. Die Doppelmembranschale wies daher genügend genaue Ergebnisse für den praktischen Gebrauch auf. Wenn jedoch ein bedeutend höherer Grad von Genauigkeit gewünscht wird, bringt das 3-Flanschen-Model eine sehr genaue Annäherung an die Lösung, die mit der Multimembranschale erhalten wurde.

Einige Kriechbeulungsversuche wurden an Zylindern aus einer Aluminiumlegierung unter verschiedenen Beanspruchungen durchgeführt. Die Zahl der ringsherum beim Bruch entstandenen Fetzen nahm mit abnehmender Belastung ab und bei einer sehr geringen axialen Mittelbeanspruchung ergab sich ein axisymmetrisches Ausbeulen.

Das in dem Bericht Nr. 100 vorgeschlagene Näherungsverfahren für die Verbeulung wurde auf die Versuchszylinder angewandt, wobei eine ziemlich gute Übereinstimmung mit den praktischen Versuchen erhalten wurde.

# DÉFORMATION PAR FLUAGE ET FLAMBAGE D'UNE VOILE CYLINDRIQUE SOUMISE À UNE COMPRESSION AXIALE

par

*Åke Samuelson*

## RÉSUMÉ

Une communication récente, le rapport n° 100 de la FFA, a établi une théorie de la déformation élastique et du fluage secondaire d'une voile cylindrique circulaire soumise à des efforts axio-symétriques, et proposé un critère approximatif du flambage. On a basé cette théorie sur l'analogie avec la « membrane *l* » et on en a tiré des solutions numériques pour le cas spécial du cylindre à double membrane. Dans le rapport actuel, les équations générales ont été résolues pour un nombre impair et arbitrairement choisi de membranes et les résultats ont été comparés avec ceux du rapport précédent.

Il est apparu que l'analogie avec la double membrane fait surestimer les taux de déformation et d'efforts, mais l'effet qu'elle provoque sur le temps de flambage par fluage, tel qu'il a été calculé par la méthode approximative, est faible par rapport à la dispersion normalement obtenue lors des expériences de flambage par fluage. On a trouvé par conséquent que la voile à double membrane fournit des résultats suffisamment précis pour les usages pratiques. Cependant, quand on veut obtenir un plus grand degré d'exactitude, le modèle à trois ailettes permet d'approcher très près de la solution fournie par la voile à plusieurs membranes.

Quelques expériences pratiques de flambage par fluage ont été réalisées sur des cylindres minces en alliage d'aluminium à différentes intensités d'effort. On a constaté que le nombre d'ondes périmétriques qui se forment au moment du gauchissement, diminue avec l'abaissement du niveau des efforts. Pour un effort axial moyen très bas, la configuration du flambage est axio-symétrique.

Le processus approximatif de flambage proposé dans le rapport n° 100 de la FFA a été appliqué aux cylindres d'essai et une assez bonne concordance avec les résultats expérimentaux a pu être dégagée.

# CONTENTS

Blank Page

# CREEP DEFORMATION AND BUCKLING OF A CIRCULAR CYLINDRICAL SHELL UNDER AXIAL COMPRESSION AND INTERNAL PRESSURE

*by*

*Åke Samuelson*

## 1. INTRODUCTION

In a previous paper, the governing equations for the state of deflections and stresses of a circular cylindrical shell subjected to secondary creep were derived. The external loads considered were uniform axial compression and constant internal or external pressure. Only axially symmetrical deformations were assumed to occur, and therefore the resulting equations depended on the coordinate $x$ along a shell generator only. In order to be able to solve the problem, the "multi-membrane" analogy was proposed. The shell was substituted for an equivalent multi-membrane shell, where a membrane was supposed to carry normal forces in its own plane only, the stresses being constant across each membrane. The membranes were connected by a core capable of carrying shear forces only. The equations were solved numerically for a few combinations of external loads and boundary conditions in the special case of a double membrane shell.

A few possible extensions of the calculations were discussed in the paper. It was pointed out that a considerable error might have been introduced by the use of the double membrane analogy. It was supposed that a few calculations using various numbers of membranes might yield an estimate of the degree of approximations which are introduced in the double-membrane case.

In the present paper, the general system of equations for such a multi-membrane shell is derived, the only limitation being the condition that the number of membranes must be odd.

An experimental investigation of creep buckling of thin circular aluminium cylinders was described in a previous paper. A few more tests have been carried out since then, and the results are given in the present paper.

## 2. LIST OF SYMBOLS

| | |
|---|---|
| $R$ | Radius of middle surface, mm. |
| $L$ | Length of shell, mm |
| $h$ | Wall thickness, mm |
| $j$ | Membrane number |
| $\Delta_j$ ($\Delta h_j$) | Thickness of membrane No. $j$. |
| $\delta_j$ | Distance between membrane No. $j$ and middle surface, mm. Positive outwards |
| $b$ | Distance between two adjacent membranes |
| $l$ | Total number of membranes |
| $k$ | Middle membrane |
| $u$ | Axial displacement, mm |
| $w$ | Radial displacement, mm |
| $E$ | Modulus of elasticity, kg/mm$^2$ |
| $\nu$ | Poisson's ratio |
| $k$, $n$ | Constants of the creep law, Eq.(1) |
| $\sigma$ | Stress, positive in tension, kg/mm$^2$ |
| $\varepsilon$ | Strain, positive in tension |
| $I$ | Second invariant of the stress deviation tensor |
| $s_{ij}$ | Stress deviation component |
| $x$, $y$, $z$ | Coordinate system, Fig. 2 |
| $\varphi$ | Circumferential direction |
| $t$ | Time |
| $\Delta x$ | Step length in the $x$-direction |
| $\Delta t$ | Step length in time $t$ |
| $M_x$,$M_\varphi$ | Local bending moments, kgmm/mm |
| $N_x$,$N_\varphi$ | Local forces in the plane of the middle surface, kg/mm |
| $T_x$,$T_\varphi$ | Local shear forces, kg/mm |

| | |
|---|---|
| $P$ | Applied axial force, kg/mm |
| $p$ | Internal pressure, kg/mm$^2$ |
| $m$ | Middle, index |
| $\mu$ | Mesh point number, index |
| $(\cdot)$ | Differentiation with respect to $t$ |
| $(')$ | Differentiation with respect to $x$ |

The dimensions of m, kg and hr were applied to the specific problems given below, but any other measuring system is applicable since the equations derived are not in any sense restricted to the given dimensions. Thus, when data are entered in the computer program, lengths and stresses, for example, may be given in in. and psi.

## 3. THEORY

The theory has been presented in Ref.[2], and the deductions will therefore be reviewed only briefly. However, a few extensions are introduced, which may be of use later on. Thus, the axial load and the external pressure are allowed to vary slowly with time, and the axial displacement $u$ is calculated in addition to the radial displacement $w$.

### 3.1. *Assumptions*

The assumptions are the same as those made in Ref. [2]:

($a$) The deflections, axial and radial, are axisymmetrical up to the time when buckling occurs.
($b$) The radial deflections are small in the prebuckling stage.
($c$) The radial stresses are small.
($d$) Deformations are caused by elastic strain and secondary creep.
($e$) Plane sections remain plane.

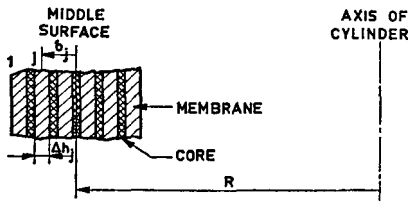


Fig. 1. Definition of the multi-membrane model.

($f$) The real shell may be replaced by an idealized multi-membrane shell according to Fig. 1. Each membrane ($j$) has the thickness $\Delta j$ and is placed a distance $\delta_j$ from the middle surface of the shell. It is supposed to carry forces in its own plane only. The number ($l$) of membranes should be odd. The core that separates the membranes is infinitely rigid against shear forces but carries no load in its own plane.

### 3.2. *Coordinate system*

The definition of the coordinate system is given in Fig. 2.

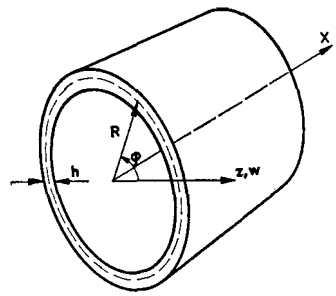


Fig. 2. Coordinate system.

### 3.3. *Relation between stress, strain, and strain rate*

The creep law is given in the unidirectional case by:

$$\dot{\varepsilon} = \frac{\dot{\sigma}}{E} + k \cdot \sigma^n \tag{1}$$

In the general case it may be written as:

$$\dot{\varepsilon}_x = \frac{1}{E}(\dot{\sigma}_x - \nu(\dot{\sigma}_\varphi + \dot{\sigma}_z)) + \frac{3k}{2}(3I)^{(n-1)/2} s_x \tag{2}$$

### 3.4. *Conditions of equilibrium*

According to Section 4.3. in Ref. [2], and Figs. 3 and 4, equilibrium in the axial and radial directions, respectively, yield:

$$N_x = -P(t) \tag{3}$$

$$pR - N_\varphi - PRw'' - RT'_x = 0 \tag{4}$$

Moreover, Fig. 4 gives the condition of momentum equilibrium:

$$M'_x = T_x \tag{5}$$

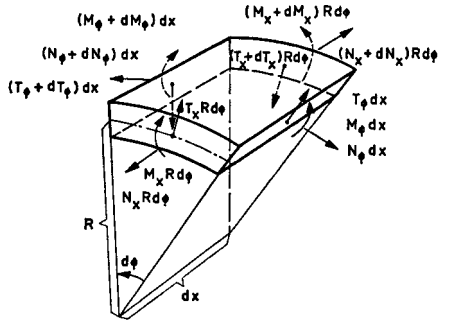


Fig. 3. Definition of the system of internal forces.

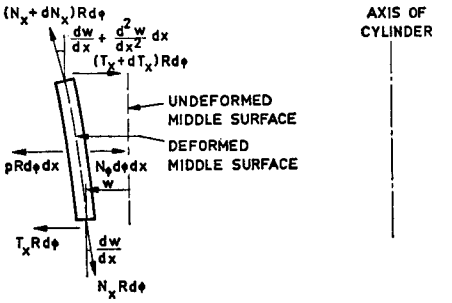


Fig. 4. Forces acting in the radial direction.

(4) and (5) yield

$$N_\varphi - pR + PRw'' + RM_x'' = 0 \tag{6}$$

### 3.5. *Deflections*

From assumption No. 5 and Fig. 5, the relations between the strains and the deflections are deduced:

$$w'' \cong -\frac{1}{z}(\varepsilon_{x1} - \varepsilon_{x0}) \tag{7}$$

$$0 \cong -\frac{1}{z}(\varepsilon_{\varphi 1} - \varepsilon_{\varphi 0}) \tag{8}$$

$$\varepsilon_{\varphi 0} = \frac{w}{R} \tag{9}$$

$$\varepsilon_{x0} = u' \tag{10}$$

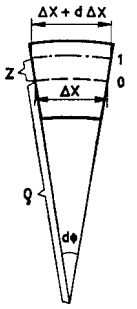


Fig. 5. Deformation of a shell element.

### 3.6. *Elastic deflections and stresses*

Eqs. (2) to (10) yield the following differential equation for the deflection $w(x)$:

$$w^{IV} + \frac{P}{D}w'' + \frac{Eh}{R^2D}w = \frac{\nu P}{RD} + \frac{p}{D} \tag{11}$$

The solution is given in the case of a fairly long clamped or simply supported cylindrical shell:

($a$) Clamped edges:

$$w = w' = 0 \text{ at } x = 0,\ L$$

$$w = w_0\left\{1 - e^{-\alpha x}\left(\frac{\alpha}{\beta}\sin\beta x + \cos\beta x\right) - e^{\alpha x}\left(\frac{\beta\sin\beta L - \alpha\cos\beta L}{\beta}\sin\beta x + \frac{\alpha\sin\beta L + \beta\cos\beta L}{\beta}\cos\beta x\right)e^{-\alpha L}\right\} \tag{12}$$

($b$) Simply supported edges:

$$w = M_x = 0 \text{ at } x = 0,\ L$$

$$w = w_0\left\{1 - e^{-\alpha x}\left[\frac{\alpha^2 - \beta^2}{2\alpha\beta}\sin\beta x + \cos\beta x\right] - e^{\alpha x}[(2\alpha\beta\sin\beta L - (\alpha^2 - \beta^2)\cos\beta L)\sin\beta x + ((\alpha^2 - \beta^2)\sin\beta L + 2\alpha\beta\cos\beta L)\cos\beta x] \times \frac{e^{-\alpha L}}{2\alpha\beta}\right\} \tag{13}$$

Here

$$w_0 = \frac{R^2}{Eh}\left(p + \frac{\nu P}{R}\right)$$

$$\left.\begin{matrix}\alpha\\ \beta\end{matrix}\right\} = \sqrt{\frac{1}{2}\left(\mp\frac{P}{2D} + \sqrt{\frac{Eh}{R^2D}}\right)} \tag{14}$$

$$D = \frac{Eh^3}{12(1-D^2)}$$

The moments and normal forces are

obtained from the results above through the relations:

$$M_x = Dw'' \tag{15}$$

$$M_\varphi = \nu M_x \tag{16}$$

$$N_\varphi = \frac{Eh}{R} w - \nu P \tag{17}$$

These equations describe the elastic state of stresses and strains which is obtained on load application, and forms the starting condition for the creep calculation.

### 3.7. *Creep deflections and stresses*

In Ref. [2] it was shown that Eqs. (2), (3), (6) and (7)–(9) may be combined to yield the following system of equations for a multi-membrane shell:

$$(\delta_j - \delta_i)\dot{w}'' + \frac{1}{E}(\dot{\sigma}_{xj} - \nu\dot{\sigma}_{\varphi j} - \dot{\sigma}_{xi} + \nu\dot{\sigma}_{\varphi i}) = J_i(\sigma_{xi} - \tfrac{1}{2}\sigma_{\varphi i}) - J_j(\sigma_{xj} - \tfrac{1}{2}\sigma_{\varphi j}) \tag{18}$$

$$\frac{1}{E}(\dot{\sigma}_{\varphi j} - \nu\dot{\sigma}_{xj} - \dot{\sigma}_{\varphi i} + \nu\dot{\sigma}_{xi}) = J_i(\sigma_{\varphi i} - \tfrac{1}{2}\sigma_{xi}) - J_j(\sigma_{\varphi j} - \tfrac{1}{2}\sigma_{xj}) \tag{19}$$

$$\frac{l}{R}\dot{w} - \frac{1}{E}\left(\sum_{j=1}^{l}\dot{\sigma}_{\varphi j} - \nu\sum_{j=1}^{l}\dot{\sigma}_{xj}\right) = \sum_{j=1}^{l} J_j(\sigma_{\varphi j} - \tfrac{1}{2}\sigma_{xj}) \tag{20}$$

$$\Delta\sum_{j=1}^{l}\dot{\sigma}_{xj} = -\dot{P}(t) \tag{21}$$

$$\Delta\sum_{j=1}^{l}\dot{\sigma}_{\varphi j} + PR\dot{w}'' - R\Delta\sum_{j=1}^{l}\dot{\sigma}''_{xj}\delta_j = -\dot{P}Rw'' \tag{22}$$

Now assume a given odd value for the integer $l$. The system above then takes the following form, where the integer $k$ denotes the middle membrane: $(k = (l+1)/2)$

$$\left.\begin{aligned}
&\delta_1\dot{w}'' + \frac{1}{E}(\dot{\sigma}_{x1} - \nu\dot{\sigma}_{\varphi 1} - \dot{\sigma}_{xk} + \nu\sigma_{\varphi k}) = -J_1 s_{x1} + J_k s_{xk} = H_{11}\\
&\frac{1}{E}(\dot{\sigma}_{\varphi 1} - \nu\dot{\sigma}_{x1} - \dot{\sigma}_{\varphi k} + \nu\sigma_{xk}) = -J_1 s_{\varphi 1} + J_k s_{\varphi k} = H_{12}\\
&\quad\cdots\\
&\delta_{k-1}\dot{w}'' + \frac{1}{E}(\dot{\sigma}_{xk-1} - \nu\dot{\sigma}_{\varphi k-1} - \dot{\sigma}_{xk} + \nu\dot{\sigma}_{\varphi k}) = -J_{k-1} s_{xk-1} + J_k s_{xk} = H_{k-11}\\
&\frac{1}{E}(\dot{\sigma}_{\varphi k-1} - \nu\dot{\sigma}_{xk-1} - \dot{\sigma}_{\varphi k} + \nu\dot{\sigma}_{xk}) = -J_{k-1} s_{\varphi k-1} + J_k s_{\varphi k} = H_{k-12}\\
&\delta_{k+1}\dot{w}'' + \frac{1}{E}(\dot{\sigma}_{xk+1} - \nu\dot{\sigma}_{\varphi k+1} - \dot{\sigma}_{xk} + \nu\dot{\sigma}_{\varphi k}) = -J_{k+1} s_{xk+1} + J_k s_{\varphi k} = H_{k+11}\\
&\frac{1}{E}(\dot{\sigma}_{\varphi k+1} - \nu\dot{\sigma}_{xk+1} - \dot{\sigma}_{\varphi k} + \nu\dot{\sigma}_{xk}) = -J_{k+1} s_{xk+1} + J_k s_{\varphi k} = H_{k+12}\\
&\quad\cdots\\
&\delta_l\dot{w}'' + \frac{1}{E}(\dot{\sigma}_{xl} - \nu\dot{\sigma}_{\varphi l} - \dot{\sigma}_{xk} + \nu\dot{\sigma}_{\varphi k}) = -J_l s_{xl} + J_k s_{\varphi k} = H_{l1}\\
&\frac{1}{E}(\dot{\sigma}_{\varphi l} - \nu\dot{\sigma}_{xl} - \dot{\sigma}_{\varphi k} + \nu\dot{\sigma}_{xk}) = -J_l s_{\varphi l} + J_l s_{\varphi l} = H_{l2}\\
&\frac{l}{R}\dot{w} - \frac{1}{E}(\dot{\sigma}_{\varphi 1} - \nu\dot{\sigma}_{x1} + \dot{\sigma}_{\varphi 2} - \ldots + \dot{\sigma}_{\varphi l} - \nu\dot{\sigma}_{xl}) = J_1 s_{\varphi 1} + J_2 s_{\varphi 2} + \ldots + J_l s_{\varphi l} = G\\
&PR\dot{w}'' - R\Delta(\delta_1\dot{\sigma}''_{x1} + \delta_2\dot{\sigma}''_{x2} + \ldots + \delta_l\dot{\sigma}''_{xl}) + \Delta(\dot{\sigma}_{\varphi 1} + \dot{\sigma}_{\varphi 2} + \ldots + \dot{\sigma}_{\varphi l}) = -\dot{P}Rw''\\
&\dot{\sigma}_{x1} + \dot{\sigma}_{x2} + \ldots + \dot{\sigma}_{xl} = -\frac{l\dot{P}}{h}
\end{aligned}\right\} \tag{23}$$

Here the following notations have been introduced:

$$J_i = k(3J_i)^{(n-1)/2} = k(\sigma_x^2 + \sigma_\varphi^2 - \sigma_x\sigma_\varphi)^{(n-1)/2} \tag{24}$$

$$s_{xi} = \sigma_{xi} - \tfrac{1}{2}\sigma_{\varphi i}; \quad s_{\varphi i} = \sigma_{\varphi i} - \tfrac{1}{2}\sigma_{xi} \tag{25}$$

It is preferable to eliminate the stress rates $\dot{\sigma}$ in the equations (23) above. This is easily done in the following way: If the circumferential stress rates $\dot{\sigma}_\varphi$ are eliminated from Eqs. (23) a,b; c,d; ... and so on in pairs, we obtain the following set of equations:

$$\left.\begin{aligned}
&\delta_1 \dot{w}'' + \frac{1-\nu^2}{E}(\dot{\sigma}_{x1} - \dot{\sigma}_{xk}) = H_{11} + \nu H_{12} \\
&\delta_2 \dot{w}'' + \frac{1-\nu^2}{E}(\dot{\sigma}_{x2} - \dot{\sigma}_{xk}) = H_{21} + \nu H_{22} \\
&\quad . \quad . \quad . \\
&\delta_l \dot{w}'' + \frac{1-\nu^2}{E}(\dot{\sigma}_{xl} - \dot{\sigma}_{xk}) = H_{l1} + \nu H_{l2}
\end{aligned}\right\} \quad (26)$$

The last one of Eqs. (23) yields with No. 3 from the bottom:

$$\dot{\sigma}_{\varphi 1} + \dot{\sigma}_{\varphi 2} + \ldots + \dot{\sigma}_{\varphi l} = \frac{El}{R}\dot{w} - EG - \frac{l\nu\dot{P}}{h} \quad (27)$$

Inserting this expression in the equation of equilibrium (No. 2 from the end) we find:

$$PR\dot{w}'' - R\Delta(\delta_1 \dot{\sigma}''_{x1} + \delta_2 \dot{\sigma}''_{x2} + \ldots + \delta_l \dot{\sigma}''_{xl}) + \frac{E\Delta l}{R}\dot{w} - E\Delta G - \frac{l\Delta\nu\dot{P}}{h} = -\dot{P}Rw'' \quad (28)$$

Now solve the last one of Eqs. (23) for $\dot{\sigma}_{xk}$ and insert the result in Eqs. (26):

$$\left.\begin{aligned}
&\delta_1 \dot{w}'' \\
&+ \frac{1-\nu^2}{E}(2\dot{\sigma}_{x1} + \dot{\sigma}_{x2} + \ldots + \dot{\sigma}_{xj} + \ldots + \dot{\sigma}_{xl}) \\
&= H_{11} + \nu H_{12} - \frac{l\dot{P}(1-\nu^2)}{Eh} \\
&\delta_2 \dot{w}'' \\
&+ \frac{1-\nu^2}{E}(\dot{\sigma}_{x1} + 2\dot{\sigma}_{x2} + \ldots + \dot{\sigma}_{xj} + \ldots + \dot{\sigma}_{xl}) \\
&= H_{21} + \nu H_{22} - \frac{l\dot{P}(1-\nu^2)}{Eh} \\
&\quad . \quad . \quad . \\
&\delta_l \dot{w}'' \\
&+ \frac{1-\nu^2}{E}(\dot{\sigma}_{x1} + \dot{\sigma}_{x2} + \ldots + \dot{\sigma}_{xj} + \ldots + 2\dot{\sigma}_{xl}) \\
&= H_{l1} + \nu H_{l2} - \frac{l\dot{P}(1-\nu^2)}{Eh} \\
&\qquad\qquad\qquad\qquad j \neq k
\end{aligned}\right\} \quad (29)$$

Multiply each of the equations by the coefficient of $\dot{w}''$ and add:

$$\left(\sum_{j=1}^{l}\delta_j^2\right)\dot{w}'' + \frac{1-\nu^2}{E}(\delta_1\dot{\sigma}_{x1} + \delta_2\dot{\sigma}_{x2} + \ldots + \delta_l\dot{\sigma}_{xl}) = \sum_{j=1}^{l}\delta_j(H_{j1} + \nu H_{j2}) \quad (30)$$

$$j = 1, 2, 3 \ldots k-1, k+1, \ldots l$$

Differentiating (30) twice with respect to $x$, it is possible to eliminate the stress rate terms with the aid of Eq. (28), and the final equation may be written:

$$R\Delta\left(\sum_{j=1}^{l}\delta_j^2\right)\dot{w}^{IV} + \frac{PR(1-\nu^2)}{E}\dot{w}'' + \frac{(1-\nu^2)\Delta l}{R}\dot{w} = \Delta(1-\nu^2)G + R\Delta\sum_{j=1}^{l}\delta_j(H''_{j1} + \nu H''_{j2}) + \frac{l\Delta\nu\dot{P}(1-\nu^2)}{Eh} - \frac{(1-\nu^2)\dot{P}Rw''}{E}; \quad j \neq k \quad (31)$$

The bending stiffness of the shell may be determined from the condition that the moment of inertia of the multi-membrane shell is to be the same as that of the real shell. Considering Fig. 1, it is readily seen that:

$$D = \frac{Eh^3}{12(1-\nu^2)} = \frac{E\Delta}{1-\nu^2}\sum_{j=1}^{l}\delta_j^2,$$

where $\delta_j = \frac{l-2j+1}{2}b$, yielding: (32)

$$b = \sqrt{\frac{h^3}{3\Delta\sum_{j=1}^{l}(l-2j+1)^2}} \quad (33)$$

Using (32), Eq. (31) is somewhat simplified:

$$\dot{w}^{IV} + \frac{P}{D}\dot{w}'' + \frac{Eh}{R^2D}\dot{w} = \frac{12(1-\nu^2)}{Rh^3}G + \frac{12\Delta}{h^3}\sum_{j=1}^{l}\delta_j(H''_{j1} + \nu H''_{j2}) - \frac{\dot{P}}{D}w'' + \frac{\nu\dot{P}}{RD} \quad (34)$$

If it is assumed that the deflection rate has been solved from Eq. (34), the axial stress rates are given by:

$$\dot{\sigma}_{xk} = -\frac{E}{l(1-\nu^2)}\sum_{j=1}^{l}(H_{j1} + \nu H_{j2}) \quad (35)$$

where $H_{kl} + \nu H_{k2} = 0.$

$$\dot{\sigma}_{xj} = \dot{\sigma}_{xk} + \frac{E}{1-\nu^2}(H_{j1} + \nu H_{j2} - \delta_j\dot{w}''); \quad j \neq k \quad (36)$$

Eq. (35) was obtained through adding Eqs. (26) together with the terms

$$\pm\frac{1-\nu^2}{E}\dot{\sigma}_{xk}$$

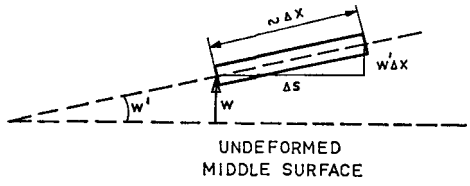


Fig. 6. Axial displacement due to rotation.

and Eq. (36) through substitution of the value thus obtained back into Eqs. (26).

The circumferential stress rates $\dot{\sigma}_\varphi$ may be calculated in the same manner. First, eliminate the $\dot{\sigma}_x$'s from the first $2(l-1)$ of Eqs. (23) and add the equations. The result is:

$$\frac{1-\nu^2}{E}\left(\sum_{j=1}^{l}\dot{\sigma}_{\varphi j}-l\dot{\sigma}_{\varphi k}\right)=\sum_{j=1}^{l}(\nu H_{j1}+H_{j2}) \quad (37)$$

where the term

$$\frac{1-\nu^2}{E}\dot{\sigma}_{\varphi k}$$

has been added and subtracted. Here again $\nu H_{k1}+H_{k2}=0$.

If now Eq. (27) is introduced into Eq. (37), the following expression is found for $\dot{\sigma}_{\varphi k}$:

$$\dot{\sigma}_{\varphi k}=\frac{E}{R}\dot{w}-\frac{EG}{l}-\frac{\nu\dot{P}}{h}$$

$$-\frac{E}{l(1-\nu^2)}\sum_{j=1}^{l}(\nu H_{j1}+H_{j2});\quad j\neq k \quad (38)$$

and with Eqs. (23):

$$\dot{\sigma}_{\varphi j}=\dot{\sigma}_{\varphi k}+\frac{E}{1-\nu^2}(\nu H_{j1}+H_{j2}-\delta_j\dot{w}'') \quad (39)$$

Finally, the axial deflection is calculated from the following equation, where the first two terms describe the axial displacement due to elasticity and creep, and the third yields the displacement due to the rotation of a shell element by $\dot{w}'$ according to Fig. 6.

$$\dot{u}'=\frac{1}{E}(\dot{\sigma}_{xm}-\nu\dot{\sigma}_{\varphi m})+\frac{1}{l}\sum_{j=1}^{l}J_j s_{xj}-w'\dot{w}' \quad (40)$$

Eqs. (34), (35), (36), (37), (39) and (40) constitute the final system of differential equations describing the behaviour of the shell during creep. The system is solved numerically by the method of finite difference approximations, as it was used in the preceding report, Ref. [2].

It may be suitable to review the procedure of calculation: On load application, elastic strains and stresses are obtained, which are calculated from Eqs. (12), or (13) and (15) to (17). The stresses of each individual membrane are given by:

$$\sigma_{xj}=\sigma_{xm}-\frac{M_x}{I}\delta_j \quad (41)$$

$$\sigma_{\varphi j}=\sigma_{\varphi m}-\frac{M_\varphi}{I}\delta_j,\quad \text{where} \quad (42)$$

$$I=\frac{h^3}{12} \quad (43)$$

$$\sigma_{xm}=-P/h \quad (44)$$

$$\sigma_{\varphi m}=N_\varphi/h \quad (45)$$

The stresses are then introduced into Eq. (34) through Eqs. (23)–(25), and Eq. (34) is solved for the deflection rate $\dot{w}$. Afterwards, the deflection rate $\dot{u}$ and the stress rates $\dot{\sigma}$ are solved from Eqs. (35), (36), (38) and (39).

This first cycle of calculation thus yields the initial state of elastic stress and strain and the stress and strain rates due to creep. An estimate of the state of stress and strain at a subsequent time $t_1=t_0+\Delta t$ is then obtained from the formula:

$$f(x,t_1)=f(x,t_0)+\Delta t\frac{\partial f}{\partial t}(x,t_0)+0(\Delta t^2) \quad (46)$$

The procedure may be repeated for as many time steps as are needed, and the result is the state of stress and strain at the time intervals $t=0,\ \Delta t,\ 2\Delta t,\ 3\Delta t,\ \ldots$

### 3.8. *Difference equations*

Using the five point formula for the second and fourth derivatives of $\dot{w}$:

$$\dot{w}''_\mu=\frac{1}{12\Delta x^2}(-\dot{w}_{\mu-2}+16\dot{w}_{\mu-1}-30\dot{w}_\mu$$

$$+16\dot{w}_{\mu+1}-\dot{w}_{\mu+2}) \quad (47)$$

$$\dot{w}_\mu^{IV} = \frac{1}{\Delta x^4}(\dot{w}_{\mu-2} - 4\dot{w}_{\mu-1} + 6\dot{w}_\mu - 4\dot{w}_{\mu+1} + \dot{w}_{\mu+2}) \quad (48)$$

and the three point formula for $H$:

$$H''_\mu = \frac{1}{\Delta x^2}(H_{\mu-1} - 2H_\mu + H_{\mu+1}) \quad (49)$$

Eq. (34) takes the form:

$$\alpha_1 \dot{w}_{\mu-2} + \alpha_2 \dot{w}_{\mu-1} + \alpha_3 \dot{w}_\mu + \alpha_2 \dot{w}_{\mu+1} + \alpha_1 \dot{w}_{\mu+2} = \Delta x^4 H_\mu \quad (50)$$

with the same notations as in Ref. [2]. $H_\mu$ is here given by:

$$H_\mu = \frac{12(1-\nu^2)}{Rh^3} G + \frac{12\Delta}{h^3 \Delta x^2} \sum_{j=1}^{l} \delta_j \times [H_{j1_{\mu-1}} - 2H_{j1_\mu} + H_{j1_{\mu+1}} + \nu(H_{j2_{\mu-1}} - 2H_{j2_\mu} + H_{j2_{\mu+1}})] - \frac{\dot{P}}{D\Delta x^2}(w_{\mu-1} - 2w_\mu + w_{\mu+1}) + \frac{\nu \dot{P}}{RD} \quad (51)$$

Eq. (50) constitutes a system of linear difference equations which are solved numerically by the same method as was used in Ref. [2]. Having obtained the deflection rates $\dot{w}_\mu$, the axial deflection rate $\dot{u}_\mu$ and the stress rates $\dot{\sigma}_\mu$ are derived from (40), (35), (36), (38) and (39), which read in the following way in difference form:

$$\dot{u}_\mu(x, t) \simeq \sum_{n=1}^{\mu} \left[\frac{1}{E}(\dot{\sigma}_{xm_n} - \nu \dot{\sigma}_{\varphi m_n}) + \frac{1}{l} \sum_{j=1}^{l} J_{j_n} s_{xj_n} - \frac{1}{\Delta x^2}(w_n - w_{n-1})(\dot{w}_n - \dot{w}_{n-1})\right] \Delta x \quad (51)$$

$$\dot{\sigma}_{xk_\mu} = -\frac{E}{l(1-\nu^2)} \sum_{j=1}^{l} (H_{j1_\mu} + \nu H_{j2_\mu}); \quad j \neq k \quad (52)$$

$$\dot{\sigma}_{xj_\mu} = \dot{\sigma}_{xk_\mu} + \frac{E}{1-\nu^2}\left[H_{j1_\mu} + \nu H_{j2_\mu} - \frac{\delta_j}{\Delta x^2}(\dot{w}_{\mu-1} - 2\dot{w}_\mu + \dot{w}_{\mu+1})\right] \quad (53)$$

$$\dot{\sigma}_{\varphi k_\mu} = \frac{E}{R}\dot{w}_\mu - \frac{EG_\mu}{l} - \frac{\nu \dot{P}}{h} - \frac{E}{l(1-\nu^2)} \sum_{j=1}^{l} (\nu H_{j1_\mu} + H_{j2_\mu}); \quad j \neq k \quad (54)$$

$$\dot{\sigma}_{\varphi j_\mu} = \dot{\sigma}_{\varphi k_\mu} + \frac{E}{1-\nu^2}\left[\nu H_{j1_\mu} + H_{j2_\mu} - \frac{\delta_j}{\Delta x^2}(\dot{w}_{\mu-1} - 2\dot{w}_\mu + \dot{w}_{\mu+1})\right] \quad (55)$$

The FORTRAN IV program is given in the appendix together with a brief description.

## 4. THEORETICAL RESULTS

A number of calculations were carried out in order to demonstrate theoretically the behaviour of a multi-membrane shell under various conditions of shell geometry, loading, boundary conditions, and integrational variables, such as the number of membranes and the step lengths in the difference equations.

### 4.1. *Influence of the number of membranes*

Four calculations were carried out for a thin cylinder under pure axial compression, where the numbers of membranes were 2, 3, 5 and 11, respectively. The results of the first, second, and last calculations are given in Figs. 7–9, and the deflections and stresses at the time $t = 1.6\ h$ are plotted in Fig. 10 for comparison. The calculations are identical except for the number of membranes.

It will be seen that the deflection and stress rates are functions of the number of membranes, the double membrane yielding the highest values. However, the differences are not very great, and in the present examples, a difference of approximately 30% is found between the maximum radial deflections as obtained with the 2- and 11-membrane shells after 1.6 hours. As a higher number of membranes is supposed to yield a better estimate of the real state of stress and strain in a creeping shell, it should be justifiable to use the double membrane analogy in creep calculations, especially as an over-estimate of the stress and strain rates will then result.

The solution approaches an asymptotic distribution very rapidly when the number of membranes is increased. This is evident from Figs. 10 and 11. In the latter of these

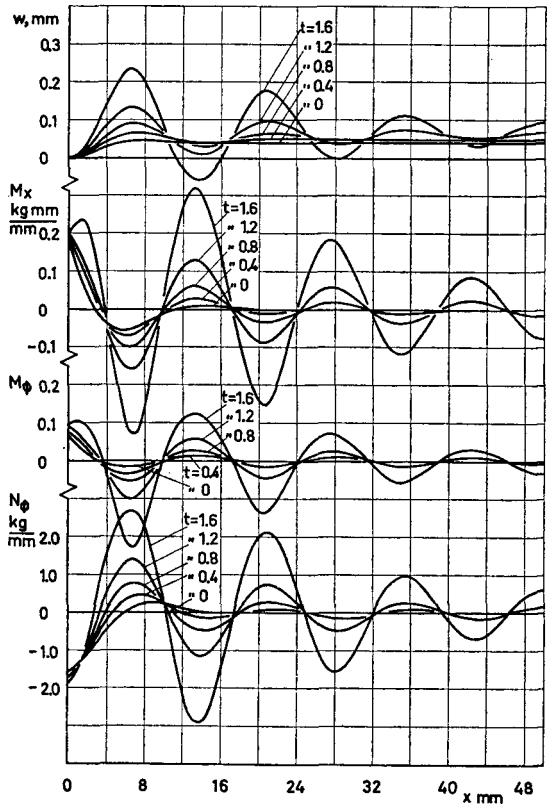


Fig. 7. Deflections and stresses of a double membrane shell as functions of the time. $h = 0.4$, $\sigma = 12$.

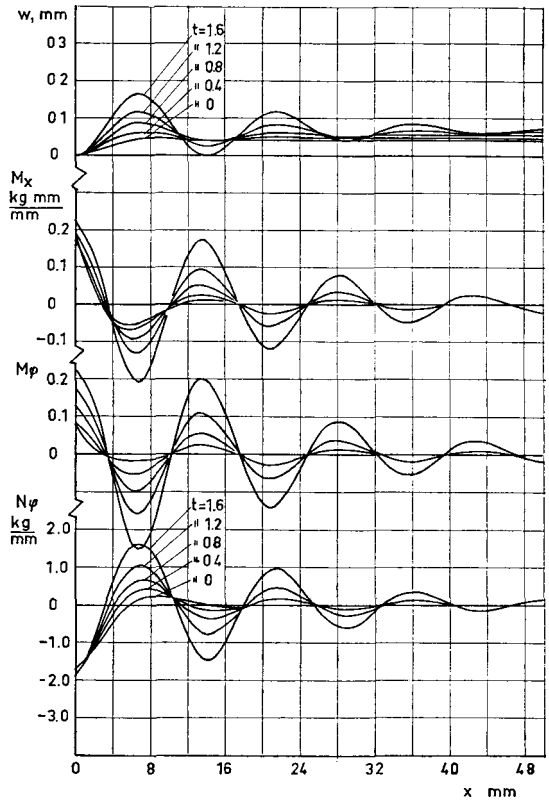


Fig. 8. Deflections and stresses of a 3-membrane shell. $h = 0.4$, $\sigma = 12$.

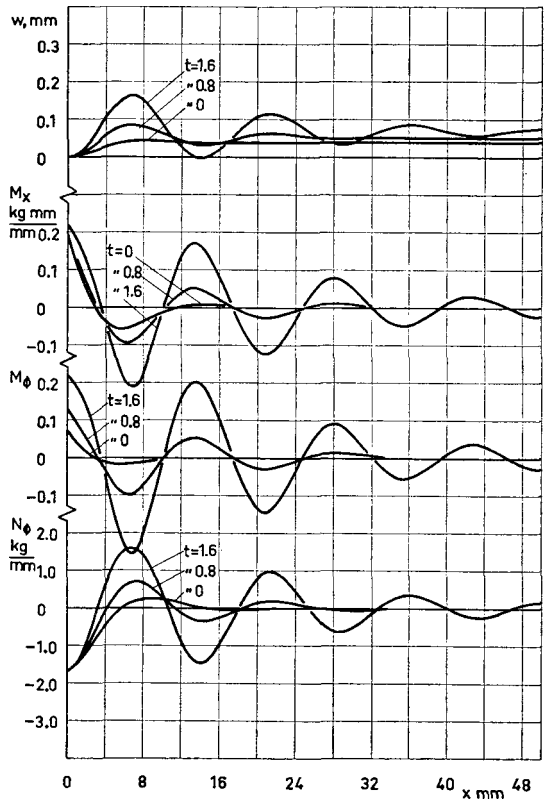


Fig. 9. Deflections and stresses of an 11-membrane shell. $h = 0.4$, $\sigma = 12$.

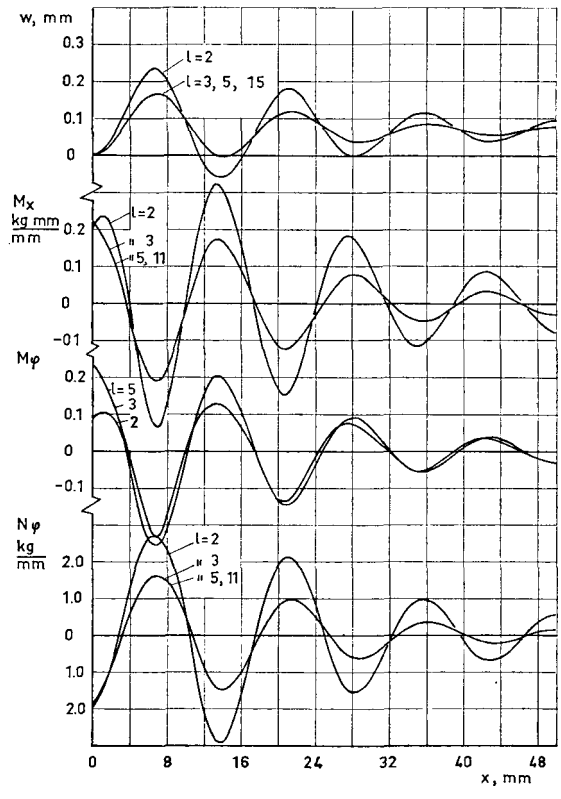


Fig. 10. Comparison between the deflections and stresses of a 0.4 mm shell at the time $t = 1.6$, obtained with different numbers of membranes.

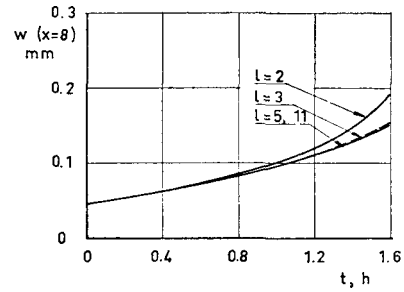


Fig. 11. The maximum deflections of Figs. 7–9 plotted as functions of the time.

figures, the peak values of the deflections are plotted as functions of the number of membranes. Practically, the asymptotic values are reached with only three membranes.

The wave length of the solution does not vary much with the number of membranes, which is rather natural if it is considered that the left hand side of Eq. (50) does not depend on $l$.

Although the solutions are similar, there are slight differences in the shape of the

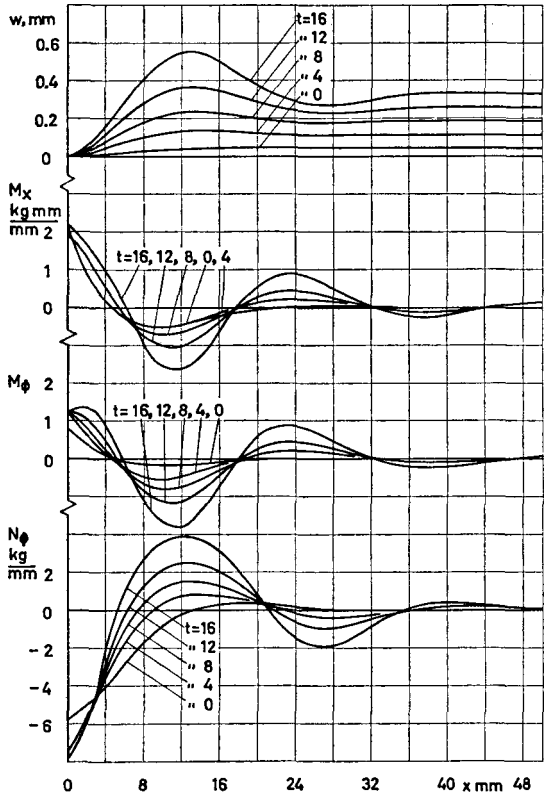


Fig. 12. Deflections and stresses of a double membrane shell as functions of the time. $h = 1.4$, $\sigma = 12$.

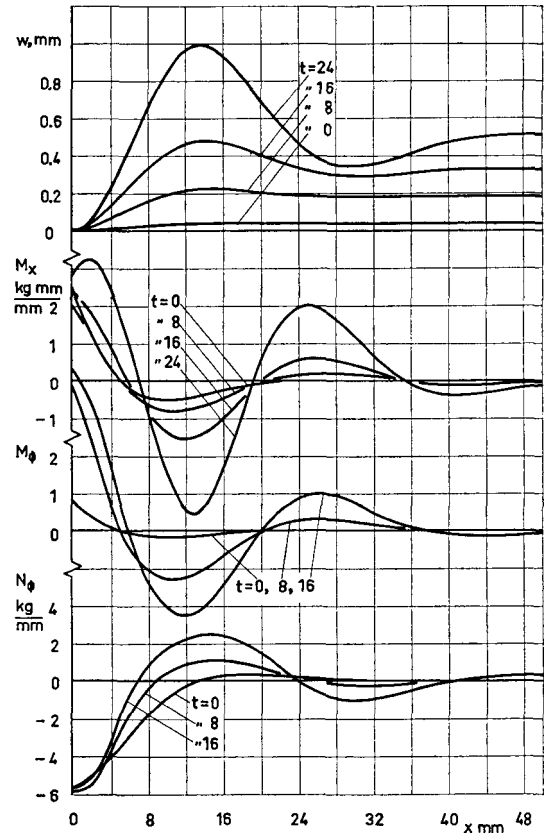


Fig. 13. Deflections and stresses of an 11-membrane shell. $h = 1.4$, $\sigma = 12$.

curves, especially in a region close to the edges. It appears that the bending moments of the double membrane solution do not increase as rapidly at the boundary as further out along a generator. In the multi-membrane solutions, however, they are higher at the boundary during the period covered by the calculation. The same result was obtained for a thicker cylinder, as can be seen in Figs. 12 and 13.

## 4.2. *Stress distribution*

The stress distribution at a few points of the shell of Fig. 9 are demonstrated in Fig. 14. It is interesting to notice that the curves are very nearly straight lines except in the neighbourhood of the boundary. This might not have been expected as the creep law used in the calculations is highly non-linear ($n = 5.8$).

The linearity is, however, dependent on the radius to thickness ratio of the shell, and

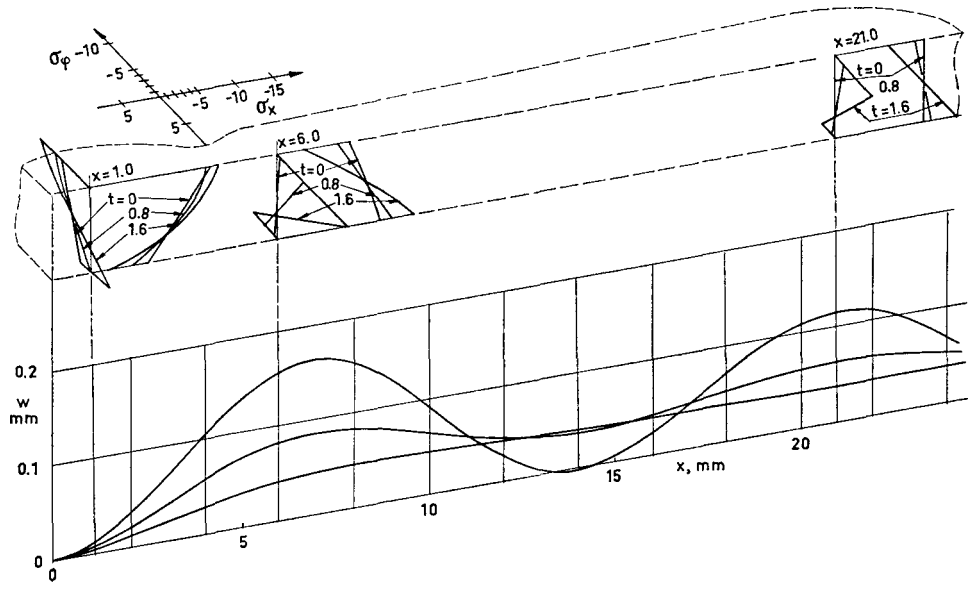


Fig. 14. Stress distributions at a few $x$-stations of the 0.4 mm shell of Fig. 9. Number of membranes $l = 11$.

for the thicker shell of Fig. 13, the stress distributions of Fig. 15 were obtained. It may be noticed that these are more curved than those depicted in Fig. 14, which in part is a consequence of the fact that the creep time is greater.

The deviations from linearity in the stress distribution are so small that the assumption of linearity may be justified when a problem of creep is treated by the use of energy or energy dissipation methods, at least in the regions where the creep deflections are of the same order of magnitude as the elastic deformations.

### 4.3. *Time dependent load*

In most of the practical cases of creep in a cylindrical shell, load and temperature vary with time. Here the variation of the load is considered only, but the two variables have similar influences on the creep deflections and stresses.

A frequently occurring loading case is stress relaxation due to creep. Then the load

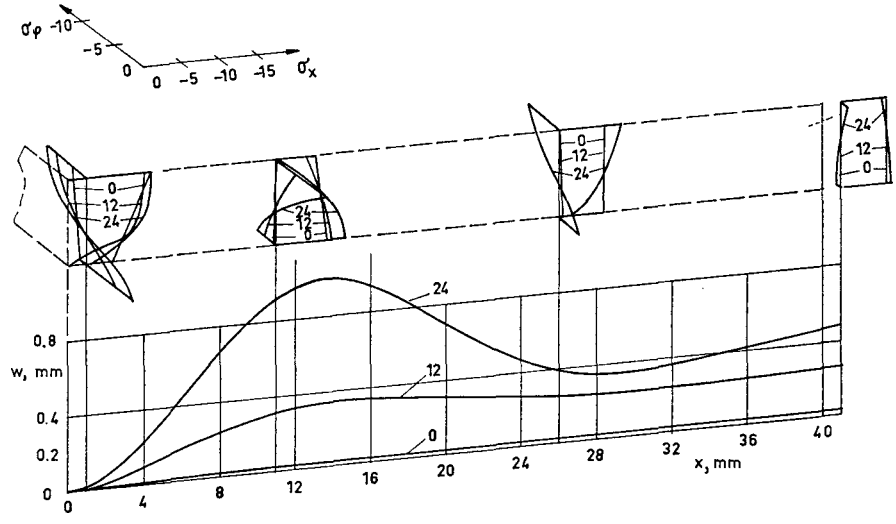


Fig. 15. Stress distributions at a few $x$-stations of the 1.4 mm shell of Fig. 13. Number of membranes $l = 11$.

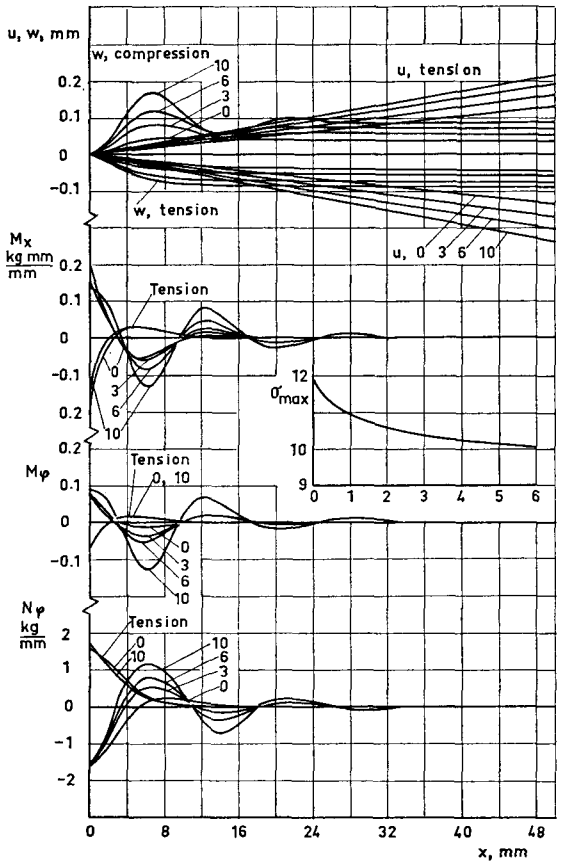


Fig. 16. Deflections and stresses of a double membrane shell subjected to a varying axial force. $h = 0.4$.

decreases with time, as the boundary conditions require that the total elongation of the shell is zero. A similar case is presented in Fig. 16, where the axial load decreases rapidly at the start and approaches an asymptotic value within some time. It is evident that the result does not differ much from that obtained with a constant axial load.

## 5. EXPERIMENTAL RESULTS

An experimental investigation of the creep behaviour and buckling of cylindrical shells under axial compression was described in Ref. [1]. Cylinders with radius to thickness ratios varying between 30 and 150 were exposed to creep at a few relatively high stress levels, and the time until buckling occurred was observed. Thus the dependence of the creep buckling time on the geometry of the shell and the load was mapped within a certain domain. It was pointed out, however, that an extension of the series of tests was under preparation, where shells of a given geometry were to be exposed to highly different stress levels. These tests have now been carried out, and the results are presented below.

### 5.1. *Testing equipment*

The tests were performed in the same loading device and furnace as were used in the previous series and are described in Ref. [1]; the reader is therefore referred to that report for further details.

The test specimens, machined from a tube of Swedish made 51S-T aluminium alloy, are depicted in Fig. 17. This tube and those used in the previous test series were not taken from the same batch of material. The creep properties are therefore not identical, and the constants of Eq. (1) are different. By the use of Fig. 18, an approximate creep law may be established as:

$$\dot{\varepsilon} = \frac{\dot{\sigma}}{5800} + 0.835 \times 10^{-8} \sigma^{4.75}, \qquad E_0 = 2800, \quad \sigma = 4 \tag{56}$$

$$\dot{\varepsilon} = \frac{\dot{\sigma}}{5200} + 0.835 \times 10^{-8} \sigma^{4.75}, \qquad E_0 = 3000, \quad \sigma = 6 \tag{57}$$

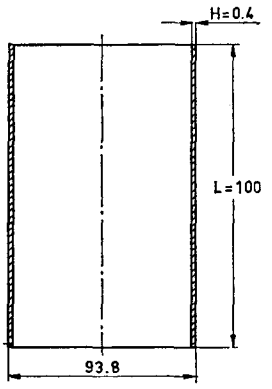


Fig. 17. Creep buckling test specimen.

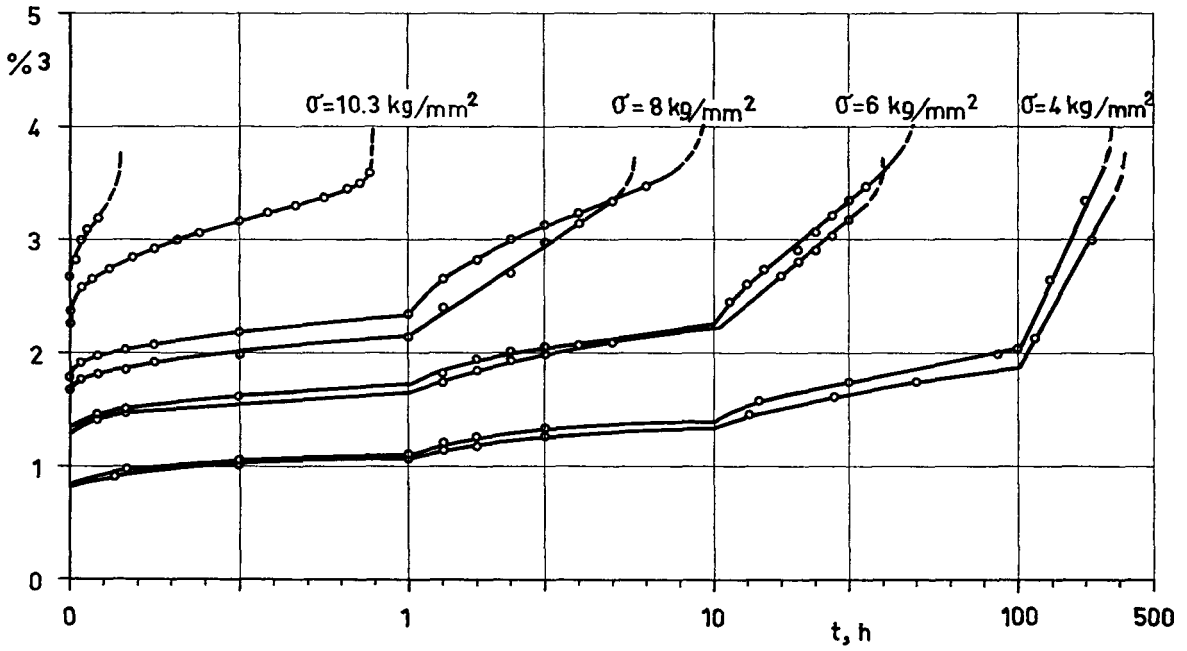


Fig. 18. Results of the 8 creep buckling experiments.

$$\dot{\varepsilon} = \frac{\dot{\sigma}}{4700} + 0.835 \times 10^{-8} \sigma^{4.75}, \qquad E_0 = 3500, \quad \sigma = 8 \qquad (58)$$

$$\dot{\varepsilon} = \frac{\dot{\sigma}}{4200} + 0.835 \times 10^{-8} \sigma^{4.75}, \qquad E_0 = 3700, \quad \sigma = 10.3 \qquad (59)$$

## 5.2. *Scope of investigation*

A total of 8 creep buckling tests were carried out. The temperature was held at a constant level of 225°C, and four levels of axial stress were applied, namely 4, 6, 8 and 10.3 kg/mm², two tests at each stress level. The load was also constant through each test.

As the primary object of the investigation was to determine the creep buckling time, only the total end shortening of the test specimens was measured, in order to be able to map the creep properties of the material.

No automatic registration of the time of collapse was employed. In some of the tests buckling occurred at night, or during a week-end, which means that the values obtained for some of the creep buckling times may contain an error of about 10%.

## 5.3. *Time of creep buckling*

The creep curves for the 8 tests are presented in Fig. 18. It may be noticed that the scatter between the pairs of tests at the same load is of a moderate magnitude, as was also the case in Ref. [1]. The creep buckling times are listed in Table 1. It may be noticed that $\log t_{cr}$ seems to be a linear function of the stress level $\sigma$. The point corresponding to the stress $\sigma = 10.3$ lies slightly under the line that can be drawn through the rest of the experimental points. This is, however, explained by the fact that this stress level is close to the yield point of the material and a lower buckling stiffness should be expected.

## 5.4. *Modes of buckling*

The cylinders of the configuration under consideration were in the previous investigation found to develop 7 circumferential buckles on collapse. The same result was obtained in the present tests for the two higher load levels, whereas only 6 buckles appeared at the load levels of 6 and 4 kg/mm². Moreover, one of the cylinders loaded at 4 kg/mm² developed an axi-

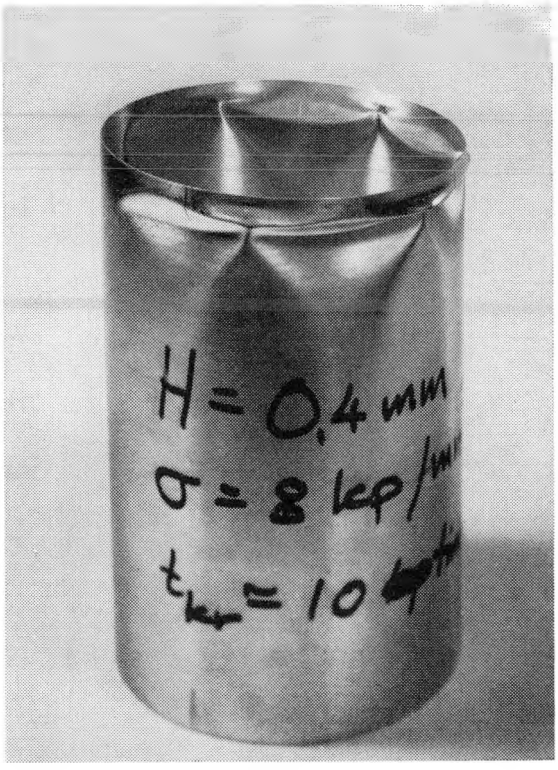


Fig. 19 a.

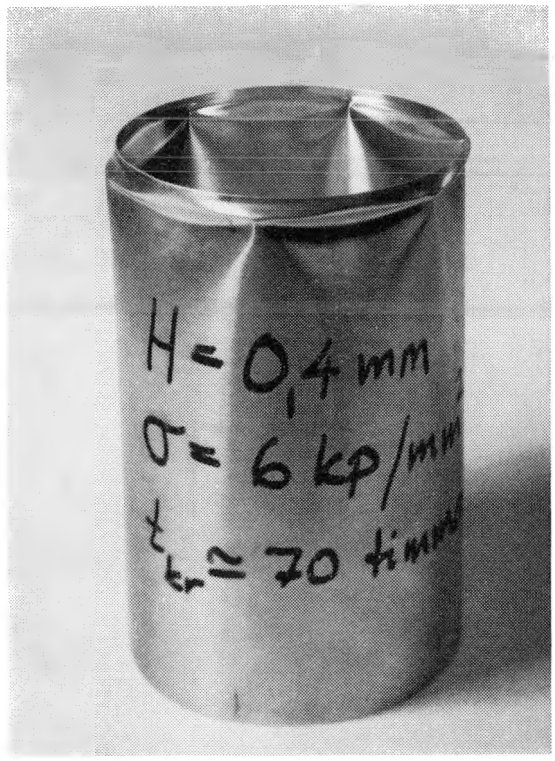


Fig. 19 b.

symmetrical buckle pattern over about 1/3 of the circumference. This is illustrated in Fig. 19, where three of the test specimens are depicted.

## 6. COMPARISON BETWEEN THEORY AND EXPERIMENTS

An approximate approach to the estimation of a critical time for a circular cylinder subject to creep under an axial load was given in Ref. [2]. The considerations were based on the assumption that buckling occurs when the maximum radial deflection reaches some critical value, which may be determined from the classical buckling theory of elastic shells. The method seemed to yield fairly good agreement between theoretical and experimental results.

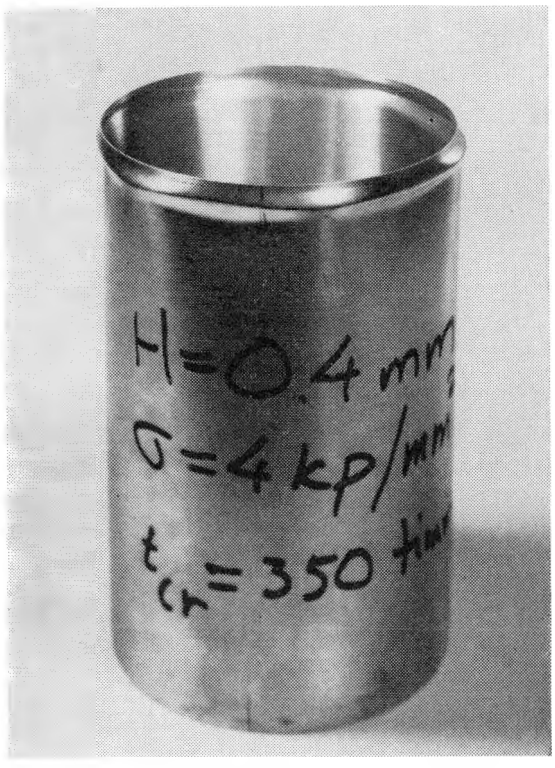


Fig. 19 c.

Fig. 19. Post buckling deformations of three cylinders subjected to 8, 6 and 4 kg/mm², respectively. The numbers of circumferential lobes are 7, 6 and 6. Note the partially axisymmetrical deflection pattern of the last test specimen.

TABLE 1. *Experimental mean values of the creep buckling time compared with theory.* $h = 0.4$, $R = 45$, $L = 100$ mm, $T = 225°C$.

| Mean stress kg/mm² | Creep buckling time, hours | |
|---|---|---|
| | Experiment | Theory |
| 4.0 | 350 | 250 |
| 6.0 | 65 | 25 |
| 8.0 | 8.5 | 5 |
| 10.3 | 0.5 | 0.8 |

Furthermore, the number of circumferential buckles obtained on collapse was also predicted by means of the classical theory, and for the thinner shells, theory and experiments showed a fair agreement.

### 6.1. *Estimation of the creep buckling time*

By use of the creep law given in Section 5.1 and the geometrical data for the tubes used in the tests, the creep deflections were calculated for each stress level. After that the critical deflection for the cylinder under the load in question was calculated according to Ref. [2] and was compared to the previously calculated creep curve. The intersection between the two curves defined the critical time.

The theoretical and experimental values are listed in Table 1.

It is evident that the theory yields a somewhat conservative estimate of the critical time, and the differences between calculated and measured values are of the same order as those reported in Ref. [2].

### 6.2. *Estimation of the number of buckles*

The method for the prediction of the buckling behaviour of the shell as given in Ref. [2] yields the number of circumferential lobes presented in Table 2. The results of Ref. [2] are included for comparison. Apparently, the method does not describe the dependence of the buckling configuration on the applied axial load very well. The theory predicts an increase in the number of buckles as the load level decreases, a condition that is contradicted by the experimental evidence.

## 7. DISCUSSION

The improvements achieved by the use of a multi-membrane shell in comparison with the results provided by the double-membrane approximation are of a fairly modest order, and it may be stated that the double membrane analogy is to be preferred because it minimizes computational time and over-estimates the stress and strain velocities. If a higher degree of accuracy is wanted, a "3-membrane" shell should suffice as it proved to yield a result that is very close to that obtained with an "11-membrane" shell.

It was shown that the wave length of the stress and deflection curves does not vary significantly with the number of membranes. The discrepancy noted in Ref. [2] between the measured wave length and that predicted by the theory thus still prevails, and should be attributed to the creep law chosen here. A better estimate should be obtained if the primary creep term is added to Eq. (1).

In Ref. [4], Rabotnov describes a method of solution for the problem of a double-layered cylindrical shell under axisymmetrical loading conditions and subjected

TABLE 2. *Number of circumferential buckles of a 0.4 mm cylinder as a function of the load level.*

| Mean stress kg/mm² | Number of buckles | |
|---|---|---|
| | Experiments | Theory |
| 4.0 | 6[a] | 9 |
| 6.0 | 6 | 9 |
| 8.0 | 7 | 9 |
| 10.0 | 7 | 8 |
| 10.3 | 7 | 8 |
| 11.0 | 7 | 8 |
| 12.0 | 7 | 6 |

[a] One of the cylinders developed an axi-symmetric mode of buckling over part of the circumference.

to stationary creep. The solution is attained through the use of a potential function and a variational method is applied in order to establish an approximate solution. This solution is assumed to be of the same type as that given by the equations of an elastic shell. No examples were given in the paper and thus it is somewhat laborious to work out a specific solution in order to carry out a comparison with the present method.

Byrne and Mackenzie, Ref. [5], carried out an investigation on essentially the same subject as Rabotnov, but they did not impose the restriction of a double membrane shell and set up the governing equations in a direct way. However, the dependence of the rates of strain and curvature was based upon the relations proposed in Refs. [9] and [10], which in fact lead to approximations analogous to those provided by the double layer model. The equations were solved by means of finite difference methods, the results showing good agreement with those of Refs. [2] and [7].

A recent report on the present subject by Diamant, Ref. [6], utilized a different creep law based on the time or strain hardening concept in order to account for primary creep. The results obtained are in many respects the same as those obtained here as far as the distributions of deflections and stresses are concerned. As the deductions are based on a different creep law, the results are not directly comparable, however, and may in a way be regarded as two solutions valid for different intervals of the creep life of a cylinder, the material of which features both primary and secondary creep.

Ref. [8] describes an experimental investigation of creep buckling of circular cylindrical shells under axial compression, where radius to thickness ratios of substantially higher values than those of Ref. [1] were used. The buckling configuration obtained differed from that of Ref. [1] and the present report as the buckles developed far away from the edges. This fact indicates that the theory of the present report (and Ref. [2]), which is based on the growth of the stress concentrations at the edges, is not applicable in that case. Evaluation of the creep lifetime of cylindrical shells of very high radius to thickness ratios must be based on a theory that takes into account the initial imperfections of the shell, which will increase with time due to creep and induce buckling. As the load level must be very low (low buckling strength), the perturbations caused by the boundaries may be considered negligible for such thin shells.

## 8. CONCLUSIONS

The multi-membrane analogy was applied to the problem of a circular cylindrical shell under secondary creep, subjected to a uniform axial compressive force, and the system of equations was solved numerically using 2, 3, 5 and 11 membranes.

It appeared that, all other parameters being held constant, the deflection rate became greater with a decreasing number of membranes. The difference in the maximum deflection was of the order of 30% between the 2 and 3-membrane solutions in a specific example, and a further increase of the number of membranes seemed to yield only a few per cent extra accuracy. In any case, 3 membranes gave a fully tolerable error level.

The use of the double-membrane analogy for the computations should be preferred as it gave an overestimate of the deflection and stress rates. It thus counteracts the effect of choosing a large steplength in time, and minimizes the computer time.

The stress distribution through the wall thickness was studied in the special case of two 11-membrane shells. It was found that the stress curves of the thinner shell at a number of $x$-stations were all practically linear during a large part of the creep life of the cylinder, the only exception being the highly stressed area in the neighbourhood of the clamped edge. An essential component of non-linearity was found to develop only after the critical time that was predicted from the approximate buckling condition.

However, the thicker shell showed highly non-linear stress distributions.

These observations seem to justify the assumption of a linear stress distribution which is frequently done in the creep analysis of plates and shells by the use of energy and energy dissipation methods, at least in the cases where the creep and elastic deflections are of the same order of magnitude. An example of this kind of investigation was provided in Ref. [3].

An experimental investigation of the creep buckling behaviour of 8 geometrically identical cylinders subjected to highly different load levels showed that the logarithm of the creep buckling time is a nearly linear function of the applied axial compressive stress level. This fact might have been anticipated, as the creep rate is a power function of the stress, and a reasonably small variation of the initial deformation level (elastic deformations on load application) has a modest influence on the critical time, as was shown for instance in Ref. [3], where the critical time was found to depend logarithmically on the initial deflection.

Application of the approximate buckling criterion given in Ref. [2] gave a fair, slightly conservative estimate of the critical time.

It was shown experimentally that the number of circumferential lobes obtained on buckling is also a function of the load level, the higher the load, the higher was the number of buckles. If the classical buckling theory was applied according to Ref. [2], an increase of the number of lobes was predicted for a decreasing load level. Thus the approximate estimate of the post buckling behaviour is rather rough.

## APPENDIX: BRIEF DESCRIPTION OF THE COMPUTER PROGRAM

The computer program is essentially the same as that described in Ref. [2] from which the two routines MAIN and COEF were retained in their original form as they perform exactly the same calculations. The subroutines ZERDEF and RHANDM were rewritten so as to meet the requirements for the multi-membrane shell equations. The BUCK routine was designed to perform an upper limit check of the maximum deflection.

The feature of a time variable axial force is not included in the version of the program presented here.

The general block diagram of the flow of calculations is given in Fig. A1, and the FORTRAN IV program lists follow in Figs. A2 to A6. As the MAIN and COEF routines were described in Ref. [2], they are only listed below and the reader is referred to that report for details. The new routines are, however, described as follows:

### *Subroutine ZERDEF*

Provision has been made to take up to 11 membranes, the total number used in a separate calculation being denoted by $L$. The elastic deflections, forces and bending moments are first calculated from Eqs. (12) (or (13)) and (15) to (17). After that, the stresses of each individual membrane are determined from Eqs. (41) to (45). Control is then transferred to the subroutine RHANDM for the calculation of the right hand members according to Eq. (51).

In the FORTRAN list, Fig. A4, the following symbols are used:

| Variable: | Meaning: |
|---|---|
| L | Total number of membranes, $l$. |
| B | Distance between two consecutive membranes, Eq. (33) |
| DEL(J) | Distance between the middle surface and membrane No. $j$. |

The variables defined in statements 8 to 45 are used in Eqs. (12) or (13), and (14) to (17), the designations being fairly obvious.

In the output, both the total forces and moments and the stresses of each membrane are given at prescribed (in input) mesh points.

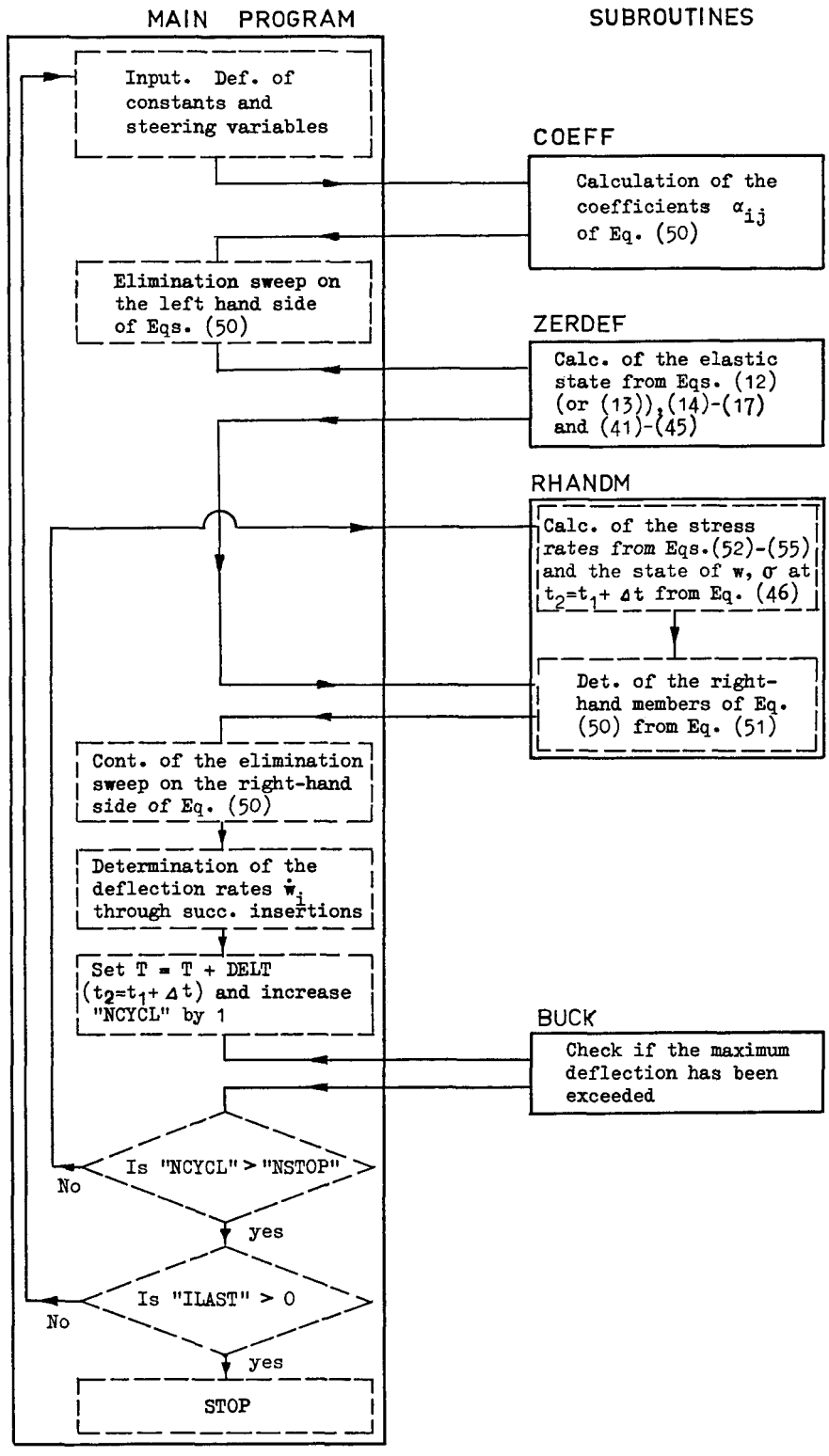


Fig. A1. Block diagram for the numerical treatment of the finite difference equations.

```
C      MAIN VERSION FOUR
C      CREEP DEFORMATION AND BUCKLING OF CYLINDRICAL SHELL
    1 DOUBLE PRECISION A
    2 DIMENSION A(499,5),H(499),V(499)
    3 COMMON A,H,V
    4 READ (5,5) NDIM,NSTOP,DELX,DELT,DTWR,ILAST,NBC
    5 FORMAT(2I3,3F5.2,2I2)
    6 EL=DELX*FLOAT(NDIM+1)
    7 WRITE (6,8) EL,DELX,DELT
    8 FORMAT(1H1,17HDATA MAIN PROGRAM/1HO,2HL=F6.2,2X5HDELX=F4.2,2X5HDEL
     1T=F5.2)
      IF(NBC) 500,500,502
  500 WRITE (6,501)
  501 FORMAT(1HO,13HCLAMPED EDGES)
      GO TO 9
  502 WRITE (6,503)
  503 FORMAT(1HO,22HSIMPLY SUPPORTED EDGES)
    9 NCYCL=1
   10 T=0.
   11 TWRIT=0.
   12 CALL COEFF(NDIM,NBC,DELX)
   13 NY=NDIM-2
   14 DO 321 L=1,NY
  114 IF(L-NY)15,115,115
  115 IF(NBC)15,15,121
   15 A(L+1,3)=A(L,4)/A(L,3)-A(L+1,3)/A(L+1,2)
   16 A(L+1,4)=A(L,5)/A(L,3)-A(L+1,4)/A(L+1,2)
   17 A(L+1,5)=-A(L+1,5)/A(L+1,2)
   18 A(L+2,2)=A(L,4)/A(L,3)-A(L+2,2)/A(L+2,1)
   19 A(L+2,3)=A(L,5)/A(L,3)-A(L+2,3)/A(L+2,1)
   20 A(L+2,4)=-A(L+2,4)/A(L+2,1)
   21 A(L+2,5)=-A(L+2,5)/A(L+2,1)
  120 GO TO 321
  121 A(L+1,3)=A(L,4)/A(L,3)-A(L+1,3)/A(L+1,2)
  221 A(L+1,4)=A(L,5)/A(L,3)-A(L+1,4)/A(L+1,2)
  321 CONTINUE
   22 A(NDIM,3)=A(NDIM-1,4)/A(NDIM-1,3)-A(NDIM,3)/A(NDIM,2)
  125 CALL ZERDEF(NDIM,NBC,T,DELX)
  126 CALL RHANDM(NDIM,NCYCL,NBC,T,TWRIT,DELX,DELT)
  226 IF(NCYCL-1000) 27,42,27
   27 DO 329 L=1,NY
  127 IF(L-NY) 28,128,128
  128 IF(NBC) 28,28,229
   28 H(L+1)=SNGL(H(L)/A(L,3)-H(L+1)/A(L+1,2))
   29 H(L+2)=SNGL(H(L)/A(L,3)-H(L+2)/A(L+2,1))
  129 GO TO 329
  229 H(L+1)=SNGL(H(L)/A(L,3)-H(L+1)/A(L+1,2))
  329 CONTINUE
   30 H(NDIM)=SNGL(H(NDIM-1)/A(NDIM-1,3)-H(NDIM)/A(NDIM,2))
   31 V(NDIM)=SNGL(H(NDIM)/A(NDIM,3))
   32 V(NDIM-1)=SNGL((H(NDIM-1)-A(NDIM-1,4)*V(NDIM))/A(NDIM-1,3))
   33 DO 435 L=1,NY
   34 J=NY+1-L
  134 IF((NDIM+1)/2-J) 35,35,135
   35 V(J)=SNGL((H(J)-V(J+1)*A(J,4)-V(J+2)*A(J,5))/A(J,3))
  235 GO TO 435
  135 V(J)=V(L+2)
  435 CONTINUE
   36 T=T+DELT
   37 IF(T-TWRIT) 40,40,38
   38 TWRIT=TWRIT+DTWR
   39 CALL BUCK(NCYCL,DELX)
   40 NCYCL=NCYCL+1
   41 IF(NCYCL-NSTOP) 126,126,42
   42 IF(ILAST) 43,4,43
   43 STOP
   46 END
```

Fig. A2. MAIN program. For description, see Ref. [2].

## *Subroutine RHANDM*

The first time the RHANDM routine is called, (NCYCL = 1), the constants needed are read in and the program constants are calculated. After that the right-hand members of Eq. (50) are evaluated. On any subsequent call, the approximate state of deflections and stresses at the time $t_{i+1} = t_i + \Delta t$ is first determined from Eq. (46) before the new right-hand members are calculated. The new FORTRAN symbols introduced in this routine, depicted in Fig. A5, are:

| Variable: | Meaning: |
|---|---|
| SX(I, J) | $\sigma_x$ of membrane No. $i$ at mesh point No. $j$. |
| SFI(I, J) | $\sigma_{\varphi_{ij}}$. |
| DEL(I) | $\delta_i$ |
| PAR(I) | $J_i$ according to Eq.(24). |
| HLI(I), HL2(I) | $H_{i1}$ and $H_{i2}$ of Eq.(23). |
| SXDOT(I), SFIDOT(I) | $\dot{\sigma}_x$ and $\dot{\sigma}_\varphi$, respectively, of membrane No. $i$. |
| H1(I, J), H2(I, J) | $H_{i1} + \nu H_{i2}$ and $\nu H_{i1} + H_{i2}$ of Eqs. (35) and (37). |
| G(J) | $G$ of Eq.(23) at mesh point No. $j$. |

```
C       SUBPROGRAM COEFF VERSION FOUR
        SUBROUTINE COEFF(NDIM,NBC,DELX)
      1 DOUBLE PRECISION A,ALFA1,ALFA2,ALFA3
      2 DIMENSION A(499,5)
      3 COMMON A
      4 READ (5,5) POI,P,E,HH,R
      5 FORMAT(2F5.2,F5.0,2F5.2)
      6 WRITE (6,7) POI,P,E,HH,R
      7 FORMAT(1H0,25HDATA SUBPR COEFF NO FOUR /1H0,4HPOI=F5.2,2X2HP=F5.2,
       12X2HE=F5.0,2X3HHH=F5.2,2X2HR=F5.2)
      8 DD=E*HH**3/(12.*(1.-POI*POI))
     10 BB=E*HH/(R*R*DD)
      9 AA=P/DD
     11 ALFA1=1.D0-DBLE(AA*DELX**2/12.)
     12 ALFA2=-4.D0+DBLE(4.*AA*DELX**2/3.)
     13 ALFA3=6.D0-DBLE(2.5*AA*DELX**2)+DBLE(BB*DELX**4)
    113 IF(NBC) 14,14,120
     14 A(1,3)=18.D0
     15 A(1,4)=-9.D0
     16 A(1,5)=2.D0
     17 A(NDIM,1)=A(1,5)
     18 A(NDIM,2)=A(1,4)
     19 A(NDIM,3)=A(1,3)
    119 GO TO 20
    120 A(1,3)=-2.D0
    121 A(1,4)=1.D0
    122 A(1,5)=0.D0
    123 A(NDIM,1)=A(1,5)
    124 A(NDIM,2)=A(1,4)
    125 A(NDIM,3)=A(1,3)
     20 N1=NDIM-1
     21 DO 26 I=2,N1
     22 A(I,1)=ALFA1
     23 A(I,2)=ALFA2
     24 A(I,3)=ALFA3
     25 A(I,4)=ALFA2
     26 A(I,5)=ALFA1
     27 RETURN
     28 END
```

Fig. A3. Subroutine COEFF, previously described in Ref. [2].

| | |
|---|---|
| N1, N2, NDEL | First and last mesh points along the shell for which $w$, $M_x$, $M_\varphi$, and $N_\varphi$ are wanted as print out. NDEL defines the step length. |
| N3, N4, N5 | The same meaning as above but defining output mesh for the stresses. |

Some further details are given in the program list.

## *Input of data*

The data cards are to be loaded in the following order, and contain the variables listed below:

| Program: | Input variables: |
|---|---|
| MAIN | NDIM, NSTOP, DELX, DELT, DTWR, ILAST, NBC |
| COEFF | POI, P, E, HH, R |
| ZERDEF | POI, P, R, HH, E, PN, N1, N2, NDEL, L, N3, N4, N5 |
| RHANDM | POI, P, R, HH, E, CR, EN, PN, N1, N2, NDEL, N3, N4, N5 |
| OUTPUT | NCH, WMAX |

The meaning if these variables is given by the list below:

| | |
|---|---|
| NDIM | Total number of mesh points, $(\text{NDIM}+1)\times\Delta x = L$. |
| NSTOP | Total number of calculation cycles to be carried out. |
| DELX | $\Delta x$ |
| DELT | $\Delta t$ |
| DTWR | Time step between output cycles. |
| ILAST | ILAST $>0$ is to be punched into the last card deck |
| NBC | NBC $\leqslant 0 \Rightarrow$ Clamped edges, NBC $>0 \Rightarrow$ Simple support. |
| E, POI | $E, \nu$. |
| EN, CR | $n$, $k$ of Eq.(1). |
| P | $P$, axial force per unit of the circumference. |
| PN | $p$, internal pressure, force per unit area. |
| R | $R$ |
| HH | $h$ |
| L | Number of flanges, $l$. Must be an odd integer. |
| N1, N2, NDEL, N3, N4, N5 | See the variable list of the RHANDM routine. |
| NCH | Number of mesh points to be checked for the condition $w > w_{\max}$, starting with $j=1$. |
| WMAX | Max. permissible radial deflection. |

```
C      CALCULATION OF THE ELASTIC DEFLECTIONS AND STRESSES OF AN
C      N-MEMBRANE SHELL IMMEDIATELY AFTER LOAD APPLICATION
       SUBROUTINE ZERDEF(NDIM,NBC,T,DELX)
     1 DOUBLE PRECISION A
     2 DIMENSION A(499,5),H(499),V(499),W(250),SX(11,251),SFI(11,251),DEL
      1(11)
     3 COMMON A,H,V,W,SX,SFI,DEL,L,B
     4 READ(5,5) POI,P,R,HH,E,PN,N1,N2,NDEL,L,N3,N4,N5
     5 FORMAT(4F5.2,F5.0,F5.3,3I3,I2,3I3)
     6 WRITE(6,7) POI,P,R,HH,E,PN,L
     7 FORMAT(1H0,25HDATA SUBPR ZERDEF NO FIVE/1H0,4HPOI=F5.2,2X2HP=F5.2,
      12X2HR=F5.2,2X3HHH=F5.2,2X2HE=F5.0,2X3HPN=F5.3/1H0,20HNUMBER OF MEM
      2BRANES=,I2)
     8 WO=R*R*(PN+POI*P/R)/(E*HH)                                          }
     9 D=E*HH**3/(12.*(1.-POI*POI))                                        } Eqs. (14)
    10 ALFA=SQRT(.5*(-P/(2.*D)+SQRT(E*HH/(R*R*D))))                        }
    11 BETA=SQRT(.5*(P/(2.*D)+SQRT(E*HH/(R*R*D))))                         }
    12 EL=DELX*FLOAT(NDIM+1)
    13 DELTA=ALFA**2-BETA**2
    14 GAMMA=2.*ALFA*BETA
   214 SIGM=P/HH
    16 C3=P*R/D
    17 MY=(NDIM+1)/2
    18 SUM=0.                                                              }
    19 DO 20 J=1,L                                                         } Det. of b from Eq.
    20 SUM=SUM+FLOAT((L-2*J+1)*(L-2*J+1))                                  } (33)
    21 B=SQRT((HH**2)*FLOAT(L)/(3.*SUM))                                   }
    22 DO 23 J=1,L                                                         } Eq. (32)
    23 DEL(J)=.5*B*FLOAT(L-2*J+1)                                          }
    24 TROEG=HH**3/12.                                                     } Eq. (43)
    25 S1=SIN(BETA*EL)                                                     |
    26 S2=COS(BETA*EL)                                                     |
    27 S3=EXP(-ALFA*EL)                                                    |
    28 IF(NBC) 29,29,34                                                    |
    29 AX=-ALFA*WO/BETA                                                    |
    30 BX=-WO                                                              |
    31 CX=-WO*(BETA*S1-ALFA*S2)*S3/BETA                                    | Det. of the elastic
    32 DX=-WO*(ALFA*S1+BETA*S2)*S3/BETA                                    | state from Eq. (12),
    33 GO TO 38                                                            | or (13) and (15) to
    34 AX=-DELTA*WO/GAMMA                                                  | (17). Calc. of the
    35 BX=-WO                                                              | coeff.
    36 CX=-WO*S3*(GAMMA*S1-DELTA*S2)/GAMMA                                 |
    37 DX=-WO*S3*(DELTA*S1+GAMMA*S2)/GAMMA                                 |
    38 AY=(DELTA*AX+GAMMA*BX)*D                                            |
    39 BY=(DELTA*BX-GAMMA*AX)*D                                            |
    40 CY=(DELTA*CX-GAMMA*DX)*D                                            |
    41 DY=(DELTA*DX+GAMMA*CX)*D                                            |
    42 AZ=C3*AY+R*(DELTA*AY+GAMMA*BY)                                      |
    43 BZ=C3*BY+R*(DELTA*BY-GAMMA*AY)                                      |
    44 CZ=C3*CY+R*(DELTA*CY-GAMMA*DY)                                      |
    45 DZ=C3*DY+R*(DELTA*DY+GAMMA*CY)                                      |
    46 WRITE(6,47) T                                                       |
    47 FORMAT(1H1,20X2HT=F6.2/1H0,3X1HX,12X1HW,13X3HEMX,12X4HEMFI,10X4HEN  |
      1FI)                                                                 |
    48 NWRIT=N1                                                            |
    49 DO 67 I=1,MY                                                        | Final evaluation of
    50 X=DELX*FLOAT(I)                                                     | the deflections and
    51 FA=SIN(BETA*X)                                                      | stresses
    52 FB=COS(BETA*X)                                                      |
    53 FC=EXP(ALFA*X)                                                      |
    54 W(I)=WO+(AX*FA+BX*FB)/FC+(CX*FA+DX*FB)*FC                           |
    55 EMX=(AY*FA+BY*FB)/FC+(CY*FA+DY*FB)*FC                               |
    56 EMFI=POI*EMX                                                        |
    57 ENFI=PN*R-(AZ*FA+BZ*FB)/FC-(CZ*FA+DZ*FB)*FC                         |
    58 DO 61 J=1,L                                                         |
    59 SX(J,I)=-SIGM-EMX*DEL(J)/TROEG                                      | Calc. of the stresses
    60 SFIO=ENFI/HH                                                        | of each membr. from
    61 SFI(J,I)=SFIO-EMFI*DEL(J)/TROEG                                     | Eqs. (41) to (45)
    62 IF(I-NWRIT)67,63,67                                                 |
    63 IF(NWRIT-N2)64,64,67                                                |
    64 NWRIT=NWRIT+NDEL                                                    |
    65 WRITE(6,66) X,W(I),EMX,EMFI,ENFI                                    |
    66 FORMAT(1H0,F7.2,4E15.5)                                             |
    67 CONTINUE                                                            |
    68 WRITE (6,69) L,L                                                    |
    69 FORMAT(1H0,///1H0,3X1HX,12X9HSX(1)-SX(,I2,1H)/1H0,24X11HSFI(1)-SFI  |
      1(,I2,1H))                                                           | Output operations
    70 DO 74 I=N3,N4,N5                                                    |
    71 X=DELX*FLOAT(I)                                                     |
    72 WRITE(6,73) X,(SX(J,I),J=1,L)                                       |
    73 FORMAT(1H0,F7.2,5E15.5/1H ,7X,5E15.5/1H ,7X,5E15.5)                 |
    74 WRITE (6,75) (SFI(J,I),J=1,L)                                       |
    75 FORMAT(1H0,12X,5E15.5/1H ,12X,5E15.5/1H ,12X,5E15.5)                |
    76 RETURN                                                              |
    77 END                                                                 |
```

Fig. A4. Subroutine ZERDEF used to calculate the elastic deflections and stresses of an *n*-membrane shell.

```
C      CALCULATION OF THE RIGHT HAND MEMBERS OF EQ.(64) IN THE
C      CASE OF AN N-MEMBRANE SHELL
       SUBROUTINE RHANDM(NDIM,NCYCL,NBC,T,TWRIT,DELX,DELT)
       DOUBLE PRECISION A
       DIMENSION A(499,5),H(499),V(499),W(250),SX(11,251),SFI(11,251),DEL
      1(11),PAR(11),HL1(11),HL2(11),SXDOT(11),SFIDOT(11),H1(11,251),H2(11
      2,251),G(251)
       COMMON A,H,V,W,SX,SFI,DEL,L,B
       IF(NCYCL-1)1,1,10
     1 READ (5,2) POI,P,R,HH,E,CR,EN,PN,N1,N2,NDEL,N3,N4,N5
     2 FORMAT(4F5.2,F5.0,E10.3,F5.2,F5.3,6I3)
       WRITE (6,3) POI,P,R,HH,E,CR,EN,PN
     3 FORMAT(1H1,25HDATA SUBPR RHANDM NO FIVE/1H0,4HPOI=F5.2,2X2HP=F5.2,
      12X2HR=F5.2,2X3HHH=F5.2,2HE=F5.0/1H0,3HCR=E10.3,2X3HEN=F5.2,2X3HPN=
      2F5.3)
       C2=12.*(1.-POI**2)*DELX**4/(R*HH*HH*FLOAT(L))
       C3=HH/FLOAT(L)
       C4=12.*DELX**2/(HH*HH*FLOAT(L))
       C10=E/((1.-POI**2)*FLOAT(L))
       C11=E/(1.-POI**2)
       C12=E/R
       SIGM=-P/HH
       EM=(EN-1.)/2.
       MY=(NDIM+1)/2
       MY1=MY+1
       NY=NDIM-1
       K=(L+1)/2
       C5=E/FLOAT(L)
       C6=1./(DELX**2)
       GO TO 50
    10 DO 17 I=1,MY
       SXDOT(K)=0.
       SFIDOT(K)=0.
       DO 11 J=1,L
       SXDOT(K)=SXDOT(K)+H1(J,I)
    11 SFIDOT(K)=SFIDOT(K)+H2(J,I)
       SXDOT(K)=-C10*SXDOT(K)
       SFIDOT(K)=C12*V(I)-C5*G(I)-C10*SFIDOT(K)
       IF(I-1) 12,12,13
    12 WBISS=C6*(-2.*V(I)+V(I+1))
       GO TO 14
    13 WBISS=C6*(V(I-1)-2.*V(I)+V(I+1))
    14 DO 15 J=1,L
       SXDOT(J)=SXDOT(K)+C11*(H1(J,I)-DEL(J)*WBISS)
    15 SFIDOT(J)=SFIDOT(K)+C11*(H2(J,I)-DEL(J)*WBISS)
       DO 16 J=1,L
       SX(J,I)=SX(J,I)+DELT*SXDOT(J)
    16 SFI(J,I)=SFI(J,I)+DELT*SFIDOT(J)
    17 W(I)=W(I)+DELT*V(I)
       IF(T-TWRIT+DELT/2.) 50,18,18
    18 WRITE (6,19) T
    19 FORMAT(1H1,20X2HT=F6.2/1H0,3X1HX,12X1HW,13X3HEMX,12X4HEMFI,10X4HEN
      1FI)
       DO 220 I=N1,N2,NDEL
       X=DELX*FLOAT(I)
       EMX=0.
       EMFI=0.
       ENFI=0.
       DO 20 J=1,L
       EMX=EMX-C3*DEL(J)*SX(J,I)
       EMFI=EMFI-C3*DEL(J)*SFI(J,I)
    20 ENFI=ENFI+SFI(J,I)*C3
   220 WRITE (6,21) X,W(I),EMX,EMFI,ENFI
    21 FORMAT(1H0,F7.2,4E15.5)
       WRITE (6,22) L,L
    22 FORMAT(1H0,///1H0,3X1HX,12X9HSX(1)-SX(,I2,1H)/1H0,24X11HSFI(1)-SFI
      1(,I2,1H))
       DO 24 I=N3,N4,N5
       X=DELX*FLOAT(I)
       WRITE (6,23) X,(SX(J,I),J=1,L)
    23 FORMAT(1H0,F7.2,5E15.5/1H ,7X,5E15.5/1H ,7X,5E15.5)
    24 WRITE (6,25) (SFI(J,I),J=1,L)
    25 FORMAT(1H0,12X,5E15.5/1H ,12X,5E15.5/1H ,12X,5E15.5)
    50 DO 51 J=1,L
       SX(J,MY+1)=SX(J,MY-1)
    51 SFI(J,MY+1)=SFI(J,MY-1)
       DO 58 I=1,MY1
       DO 53 J=1,L
       PAR(J)=CR*(SX(J,I)*SX(J,I)+SFI(J,I)*SFI(J,I)-SX(J,I)*SFI(J,I))**EM
       IF(PAR(J)-1.E+10) 53,52,52
    52 NCYCL=1000
       GO TO 67
    53 CONTINUE
       DO 56 J=1,L
       IF(J-K) 55,54,55
```

Consequent cycles

First cycle

Def. of constants used in Eq. (31) and the following

Evaluation of the stress rates from Eqs. (35), (36), (38) and (39)

Det. of the state at $t_{\mu+1}$, Eq. (46)

Local forces and moments recalc. from Eqs. (41)–(45)

Output

Eq. (24)

```
54 HL1(K)=0.
   HL2(K)=0.
   GO TO 56
55 HL1(J)=-PAR(J)*(SX(J,I)-.5*SFI(J,I))+PAR(K)*(SX(K,I)-.5*SFI(K,I))
   HL2(J)=-PAR(J)*(SFI(J,I)-.5*SX(J,I))+PAR(K)*(SFI(K,I)-.5*SX(K,I))
56 CONTINUE
   G(I)=0.
   DO 57 J=1,L
   G(I)=G(I)+PAR(J)*(SFI(J,I)-.5*SX(J,I))
   H1(J,I)=HL1(J)+POI*HL2(J)
57 H2(J,I)=POI*HL1(J)+HL2(J)
58 CONTINUE
   IF(NBC) 59,59,60
59 H(1)=0.
   GO TO 62
60 H(1)=0.
   DO 61 J=1,L
61 H(1)=H(1)+C4*DEL(J)*H1(J,1)
62 DO 66 I=2,NDIM
   IF(I-MY) 63,63,65
63 H(I)=C2*G(I)
   DO 64 J=1,L
64 H(I)=H(I)+C4*DEL(J)*(H1(J,I-1)-2.*H1(J,I)+H1(J,I+1))
   GO TO 66
65 J1=NDIM+1-I
   H(I)=H(J1)
66 CONTINUE
67 RETURN
   END
```

*H* of Eqs. (23)

Calc. of the creep terms of Eq. (34)

Def. of the right hand members corr. to the boundary conditions

Evaluation of the right hand members of Eq. (34).

Fig. A5. Subroutine RHANDM for the calculation of the right hand members of Eq. (34).

```
C     PROGRAM FOR DETERMINATION OF THE CRITICAL TIME
      SUBROUTINE BUCK(NCYCL,DELX)
      DOUBLE PRECISION A
      DIMENSION A(499,5),H(499),V(499),W(250)
      COMMON A,H,V,W
      IF(NCYCL-1) 1,1,3
    1 READ(5,2) NCH,WMAX
    2 FORMAT(I5,F10.5)
    3 DO 4 I=1,NCH
      IF(W(I)-WMAX) 4,4,6
    4 CONTINUE
      GO TO 10
    6 NCYCL=1000
      WRITE(6,7)
    7 FORMAT(1H1,23H MAX. DEFLECTION REACHED)
   10 RETURN
      END
```

Fig. A6. Subroutine BUCK. The total deflections $w_i$ are compared with a prescribed upper limit value. If this is exceeded, the calculations are interrupted.

## REFERENCES


1. Samuelson, Å.: An experimental investigation of creep buckling of circular cylindrical shells subject to axial compression. *Aero. Res. Inst. Sweden (FFA), Report No. 98* (1964).
2. Samuelson, Å.: A theoretical investigation of creep deformation and buckling of a circular cylindrical shell under axial compression and internal pressure. *Aero. Res. Inst. Sweden (FFA), Report No. 100* (1964).
3. Serpico, J. C.: A study of creep collapse of a long circular cylindrical shell under various distributed force systems. *J. Aero/Space Sci., Vol. 29, No. 11* (November 1962), pp. 1316–1323.
4. Rabotnov, Iu.N.: Axisymmetrical creep problems of circular cylindrical shells. *Prikl. Mat. Mekh., Vol. 28, No. 6* (1964), pp. 1040–1047 (Transl.: *J. Appl. Math. Mech., Vol. 28, No. 6* (1964), pp. 1255–1263).
5. Byrne, T. P., Mackenzie, A. C.: Secondary creep of a cylindrical thin shell subject to axisymmetric loading. *J. Mech. Engng Sci., Vol. 8, No. 2* (June 1966), pp. 215–225.
6. Diamant, E. S.: Axisymmetric creep in cylindrical shells. *AIAA Paper No. 66–123* (1966).
7. Cozzarelli, F. A., Patel, S. A., Venkatraman, B.: Creep analysis of circular cylindrical shells. *Polytech. Inst. Bklyn., Dept. Aero. Eng. & Appl. Mech., PIBAL Report No. 685* (1964).

8. CARLSON, R., SCHNEIDER, B., BERKE, L.: An experimental study of the creep buckling of circular cylindrical shells under an axially applied compression. *Stanford Univ., Dept. Aero. & Astron., SUDAER No. 248* (1965).
9. ROZENBLIUM, V. I.: Approximate equations of creep of thin shells. *Prikl. Mat. Mekh., Vol. 27, No. 1* (1963), pp. 154–159 (Transl.: *J. Appl. Math. Mech., Vol. 27, No. 1* (1963), pp. 217–226).
10. MACKENZIE, A. C.: On the equations for steady state creep of thin shells. *J. Mech. Engng. Sci., Vol. 7, No. 1* (March 1965), pp. 114–117.
11. KURSHIN, L. M.: An approach to the problem of buckling of a shell during creep. *Sov. Phys. Dokl., Vol. 10, No. 7* (January 1966), pp. 680–682.